International Journal of Advanced Research in Biological Sciences
ISSN: 2348-8069
www.ijarbs.com
Volume 3, Issue 4 - 2016

Research Article

SOI: http://s-o-i.org/1.15/ijarbs-2016-3-4-3

Co(II) and Cu(II) complexes of oxime hydrazone derivative: Structural, geometrical, biological studies and ion-flotation separation of Cu(II) ions.

Hany M. Youssef[1], Mohammed M. El-Gamil[2], YasirKh. Abdulhamed[1], Gaber M. Abu El-Reash[1*]

[1] Department of Chemistry, Faculty of Science, Mansoura University, Mansoura, Egypt.
[2]Department of Toxic and Narcotic Drug, Forensic Medicine, Mansoura Laboratory, Medicolegal Organization, Ministry of Justice, Egypt.

*** Corresponding author: Prof. Dr. Gaber Mohammed Abu El-Eeash**
Tel.: +201000373155; fax: +20 502219214.
*E-mail: *gaelreash@mans.edu.eg*

Abstract

Co(II) and Cu(II) complexes enclosing xime hydrazone ligand (H_4MDO) prepared via the condensation of malonohydrazide with diacetyl monoxime were synthesised and characterized using elemental analysis, magnetic and spectral measurements. The proposed tetrahedral structures of both complexes were proved using DFT optimization and conformational analysis. The thermal decomposition behaviour of complexes were discussed. Kinetic parameters (ΔH, ΔS, ΔG, E and A) of resulted thermal decomposition stages have been calculated using Coats-Redfern and Horowitz-Metzger methods. Ion-flotation separation of Cu(II) ions was carried out from aqueous solutions using oxime derivative as chelating agent and oleic acid as surfactant. H_4MDO shows the highest minimum inhibitory concentration (MIC) activity of Co(II) complex against *Staphylococcus aureus*, *Escherichia coli* and *Candida albicans*. Cytotoxicity assay of the above complexes revealed the higher activity of H_4MDO and Co(II) complex than Cu(II) complex.

Keywords: Hydrazones; Spectral characterization; thermal degradation; Ion-flotation separation; Cytotoxicity activity.

Introduction

The hydrazones derived from the dihydrazide of aliphatic acids such as oxalic and malonic acids have interesting and valuable coordination properties with metal ions, where these ligands contain various donor centers, in addition to selectivity, flexibility and sensitivity to transition metal ions[1, 2]. Furthermore, hydrazones have numerous applications in analytical chemistry as transition metal binders [3].Ion Flotation has recently received a considerable attention as a separation process regarding to its economy, rapidity, simplicity, good separation yields and the ability to apply it for many species having various structure and nature, friability and flexibility of processing and equipment for recovery purpose [4, 5].Hydrazone are found to have pharmaceutical and biological activities including antimicrobial [6, 7], inhibition of tumor growth [8, 9] and anti-tubercular [10] as well as 2-acetylpyridine benzoyl hydrazone (APBH) exhibits clear improvement in the anti-tubercular activity upon complexation with Cu(II) metal ion.[11].In continuation to our previous work [12, 13], the present work aims to synthesize and characterize Co(II) and

Cu(II) complexes of N'^1,N'^3-bis((2E,3Z)-3-(hydroxyimino) butan-2-ylidene) malonohydrazide (H_4MDO). The modes of chelation and the geometry of complexes are discussed based on the resulted(DFT) quantum calculations, magnetic measurements and the different spectroscopic methods (^1H and ^{13}C-NMR, IR, UV–visible). Moreover, the kinetics and thermodynamic characteristics of the thermal decomposition steps have been studied employing Coats–Redfern and Horowitz–Metzger models. Also their Minimum inhibitory concentration (MIC) and Cytotoxicity assay have been tested. Also, ion-flotation separation of Cu(II) ions was carried out from aqueous solutions using oxime derivative as chelating agent and oleic acid as surfactant.

Experimental

Materials and Instrumentation.

The Co (II) and Cu(II) chloride salts, diethyl malonate, hydrazine hydrate and diacetyl monoxime were of analytical grade. Oleic acid (HOL) surfactant stock solution 6.36×10^{-2}mol L^{-1}, was prepared by dispersing 20 mL in one liter of kerosene. Copper chloride ($CuCl_2$) stock solution, 1×10^{-2}mol L^{-1},was prepared in double distilled water. The stock solution of H_4MDO, 1×10^{-2}mol L^{-1}, was prepared in absolute ethyl alcohol. (C, H and N) percent in the prepared H_4MDO and complexes were detected using a Perkin–Elmer 2400 series II analyzer, while metal and chloride contents were carried out according to the standard methods[14]. Thermogravimetric (TGA) and differential thermal analysis (DTA) measurements were carried out on a Shimadzu TGA-50H thermogravimetric analyzer at temperature range (20–800^oC) with a heating rate of 10 ^oC/min and nitrogen flow rate of 15 ml/min. The standard used in the experiment is Pt. 10% Rh. A Sherwood Magnetic Balance was utilized to measure the magnetic susceptibility of solid complexes.IR spectra were recorded on a Mattson 5000 FTIR spectrophotometer in range (4000–400 cm^{-1}) using KBr discs, while Perkin Elmer Lamda 25 UV/Vis Spectrophotometer was used to record the electronic spectra of complexes in DMSO solution.^1H and ^{13}C-NMR measurements in d_6-DMSO at room temperature were carried out on Mercury and Gemini 400 MHZ spectrometer. In ion-flotation separation of Cu(II) and Co(II), All the determinations of the analytes were carried out using GBC, Sensaa Series Atomic Absorption Spectrometry (computerized AAS) with air-acetylene flame under the optimum instrumental conditions (324.7 nm as wave length, 1-5 ppm as working calibrating range with 0.025 µg/ml sensitivity). The flotation and separation cells were a glass cylinder with45 cm length and 6 cm inner diameter with a quick-fit stopper at the top and a stopcock at the bottom [15]. These cells were used to examine the separation of Cu(II) ions from 1 L of some natural water samples. The pH of studied solutions was adjusted using Hanna Instrument 8519 digital pH meter.

Synthesis of H_4MDO

The malonohydrazide was prepared by slowly adding hydrazine and diethyl malonate with ratio of (2:1) in absolute ethanol present in ice bath for 30 minutes with continues stirring. then the resultant material filtered and washed several times with absolute ethanol and dried in a vacuum desiccator over anhydrous $CaCl_2$. Known amount of prepared material mixed with diacetyl monoxime (2,3-butanedione monoxime) in presence of few drops of glacial acetic acid and the mixture was refluxed on a water bath for a time of (2-4 hours). The product thus obtained was crystallized several times from absolute ethanol and dried in a vacuum desiccator over anhydrous $CaCl_2$.

Synthesis of Complexes

A hot ethanolic solution of the respective metal chloride(1.0 mmol) was added to a hotethanolic medium of H_4MDO(0.298 g, 1.0mmol). The resultant mixture was boiled under reflux for 3– 4 h. All complexes were filtered off, then washed well with hot EtOH followed by diethyl ether and dried over anhydrous $CaCl_2$in a vacuum desiccator. The physical and analytical data are listed in (Table 1). It is clear that, prepared complexes are stable in air and have high melting points.

Table 1. Analytical and physical data of H_4MDO and its complexes.

Compound	M.wt.	Color	M.P.; °C	% Found (Calcd.)					Λ_m° Yield%
				M	Cl	C	H	N	
(H_4MDO) $C_{11}H_{18}O_4N_6$	298.3	White	218	—	—	44.90 (44.29)	6.25 (6.08)	28.74 (28.17)	97
$[Co_2(H_2MDO)Cl_2(H_2O)_2]H_2O$. $C_{11}H_{22}Cl_2Co_2N_6O_7$	539.1	Dark green	>300	21.90 (21.86)	13.74 (13.15)	24.18 (24.51)	4.58 (4.11)	15.42 (15.59)	85
$[Cu_2(H_2MDO)Cl_2(H_2O)_2]2H_2O$. $C_{11}H_{24}Cl_2Cu_2N_6O_8$	566.34	Light green	>300	22.97 (22.44)	12.33 (12.52)	23.90 (23.33)	4.79 (4.27)	14.76 (14.84)	87

Ion-Flotation Separation of Cu(II):

Flotation-Separation Procedure

A suitable aliquots containing a known amount of Cu^{2+} ions and H_4MDO ligand, specified for each investigation, were mixed together. The solution pH adjusted with HNO_3 and/or NaOH to the required value. Then, test solution transferred to the flotation cell, the total volume made up to 10 mL with deionized water and shaked well for 2 min to ensure complete complexation followed by addition of 2 mL of HOL (with known concentration). The flotation cell then inverted upside down twenty times by hand and left 5 min standing for complete flotation. Finally, the concentration of Cu^{2+} ions in the mother liquor was determined by AAS. The floatability (F %) of Cu^{2+} ions was calculated according to equation (1):

$$F\% = (C_i - C_f) / Ci \times 100 \qquad (1)$$

where: C_i and C_f denote the initial and the final concentrations of Cu^{2+} ions in the mother liquor, respectively.

Biology

Minimum Inhibitory Concentration (MIC)

The synthesized H_4MDO and its complexes tested as anti-bacterial compounds against some strains separated from animal byproducts and accused of being a main reason for food intoxication in human. Gram-positive bacteria *(Staphylococcus aureus)* and Gram-negative bacteria *(Escherichia coli)* utilized in this experiment using Muller Hinton agar medium (Oxoid). In addition, the anti-fungal properties of these compounds also tested against *(Candida albicans)* using Sabouraud dextrose agar medium (Oxoid).

Ciprofloxacin (100 µg/ml) and Fluconazole (100 µg/ml) were used as standard for anti-bacterial and anti-fungal activity.

Agar streak dilution method used to determine MIC [16]of the compounds. A stock solution of H_4MDO and complexes (100 µg/ml) prepared in DMSO, then definite amounts of the test compounds were mixed with specific quantity of molten sterile agar (Sabouraud dextrose agar medium for anti-fungal activity and Muller Hinton agar for anti-bacterial activity). A specified quantity of the medium (40—50 °C) containing the compound was poured into a Petri dish to give a depth of 3-4 mm and allowed to solidify. Micro-organism suspension contains about 105 cfu/ml applied to plates with serially diluted compounds dissolved in DMSO and incubated at 37 °C for 24 and 48 h for bacteria and fungi, respectively. The MIC considered as the lowest concentration of the test substances showing an invisible growth of fungi or bacteria on the plate.

Cytotoxicity Assay

Materials and methods

Cell line

Hepatocellular carcinoma (HePG-2), The cell line were obtained from ATCC via Holding company for biological products and vaccines (VACSERA), Cairo, Egypt.

Chemical reagents

The reagents RPMI-1640 medium, MTT, DMSO and 5-fluorouracil (sigma co., St. Louis, USA), Fetal Bovine serum (GIBCO, UK). 5-fluorouracil was used as a standard anticancer drug for comparison.

MTT assay

The cell line was utilized to decide the inhibitory impacts of compounds on cell development utilizing the MTT test[17]. Mitochondrial succinate dehydrogenase was responsible for the colorimetric change of the yellow tetrazolium bromide (MTT) to a purple formazan derivative in suitable cells. The cells were refined in RPMI-1640 medium with fetal bovine serum (10%). Antibiotics (100 units/ml penicillin and 100µg/ml streptomycin) were inserted at 37 ^oC in a 5% CO_2 incubator. The cells were seeded in a 96-well plate at a density of $1.0x10^4$ cells/well under 5% CO_2 at 37 ^oC for 48 h[18]. . After a time of incubation, the cells were treated with compounds by different concentration and incubated again for 24 h. After drug treatment (24 h), add 20 µl of MTT solution at 5mg/ml and incubated for 4 h. Add 100 µl dimethyl sulfoxide (DMSO) to each well to dissolve the formed purple formazan using a plate reader (EXL 800, USA), The colorimetric assay is recorded at an absorbance 570 nm.

$$The\ relative\ cell\ viability\% = \frac{A_{570}\ of\ Treated\ Samples}{A_{570}\ of\ Untreated\ Samples} \times 100$$

Molecular Modeling

$DMOL^3$ program used to study the cluster calculations [19] in Materials Studio package [20].Density

functional theory DFT semi-core pseudopods calculations (dspp) were done using the double numerical basis sets plus polarization functional (DNP). The DNP basis sets are of comparable quality to 6-31GGaussian basis sets [21]. It was reported previously by Delley et al. that Gaussian basis sets are less accurate than the DNP basis sets of the same size [22]. The RPBE functional is employed to take account of the exchange and correlation effects of electrons , where it is so far considered the best exchange–correlation functional [23] based on the generalized gradient approximation (GGA) [24]. The geometric optimization displayed without any symmetry limitation.

Results and Discussion

IR Spectra of H_4MDO and Complexes.

Table (2) show the most important assignments of IR spectral bands of H_4MDO and its complexes. H_4MDO(structure 1) (in KBr) shows four bands at 1694, 1668, 1603 and 936 cm^{-1} which are assigned to ν(C=O), $\nu(C=N)_{azomethine}$, $\nu(C=N)_{oxime}$ and ν(NO), respectively. The bands located at 3294 and 3208 cm^{-1} (broad) assigned to ν(OH) and ν(NH) (sym and asym), respectively. The band observed at 985 cm^{-1} is due to the ν(N-N) vibration which shifts to higher wave number upon complexation [25].

Table 2. Assignments of IR spectral bands of H_4MDO and its complexes.

Compound	ν(C=O)	υ(C=N) azo	ν(C=N) oxime	ν(NH)	υ(C=N)*	υ(C-O)*	ν (N-N)	ν (OH)	ν (M-O)	ν (M-N)
H_4MDO	1694	1668	1603	3208	-	-	985	3294	-	-
$[Co_2(H_2MDO)Cl_2(H_2O)_2]H_2O$	-	1657	1625	-	1524	1163	1024	2407	505	486
$[Cu_2(H_2MDO)Cl_2(H_2O)_2]2H_2O$	-	1621	1621	-	1585	1154	1023	3469	554	470

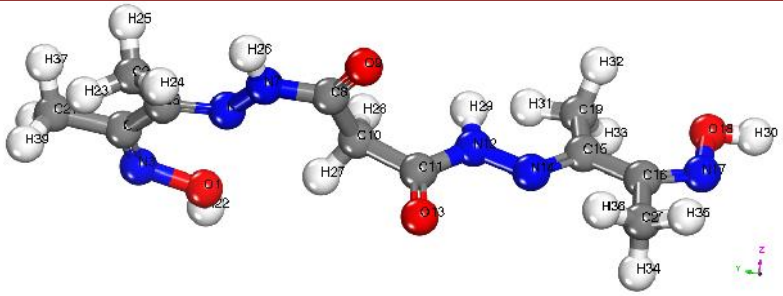

Structure 1.Molecular modeling of H_4MDO

In the binuclear complexes of Co(II) (structure 2) and Cu(II) (structure 3), the H_4MDO behaves as binegative tetradentate where the spectra of complexes show the absence of the bands due to ν(C=O) and ν(NH) groups and the shift of ν(C=N) to lower frequency side (10-15 cm^{-1}) due to coordination as well as a sharp band in the vicinity of 1580 cm^{-1} was observed which can be assigned to stretching mode of chromophores ν(-C=N-N=C-) due to the enolization of (C=O).

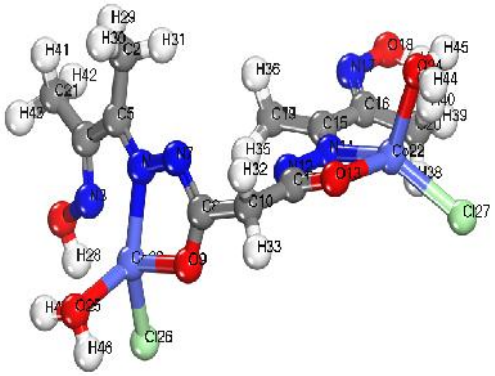

Structure 2.Molecular modeling of $[Co_2(H_2MDO)Cl_2(H_2O)_2]H_2O$

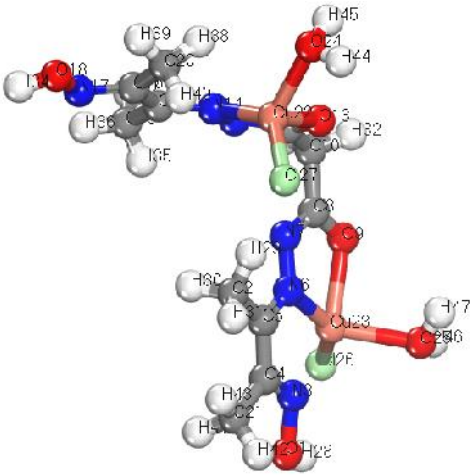

Structure 3.Molecular modeling of $[Cu_2(H_2MDO)Cl_2(H_2O)_2]2H_2O$

^{1}H and ^{13}C-NMR Spectra of the H_4MDO.

The ^{1}H-NMR spectrum of H_4MDO in d_6-DMSO solution (fig. 1) shows signals at δ=11.48 ppm (s,1H) and 10.66 ppm (d,1H) assignable to protons of $(OH)_{oxime}$ and (NH) groups, respectively. The two signals are disappeared upon addition of D_2O. The signals attributed to the methyl protons (12H) appeared at 1.891 and 2.058 ppm while the signal at 3.429 ppm attributed to methylene (CH_2) protons.

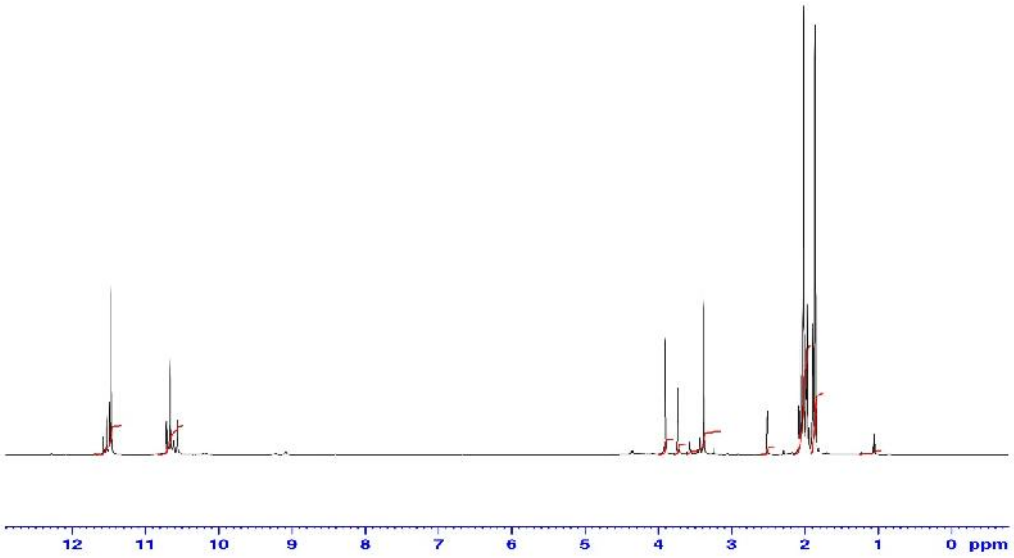

Fig. 1. ^{1}HNMR spectra of H_4MDO

In the ^{13}C-NMR (fig. 2) the signals at 170.58 ppm due to (C=O) and the signals at 164.05 and 155.15 ppm assigned to $(C=N)_{azomethine}$ and (C=NOH) syn (oxime). The signals at 147.13 ppm attributed to (C=NOH)anti (oxime).

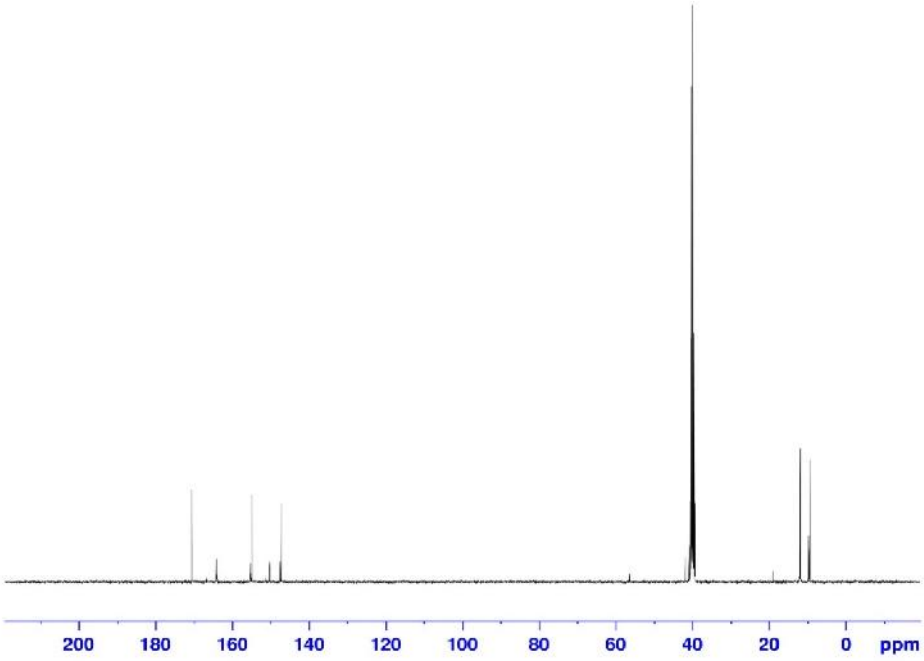

Fig. 2. ^{13}CNMR spectra of H_4MDO

Electronic Spectral and Magnetic Moments Studies

The electronic spectral bands of H_4MDO and its complexes are listed in (Table 3).The spectrum of H_4MDOshow an intense absorption bands bands at 42735, 39682, 33783 and 25510 cm^{-1}assignable to $(\pi \rightarrow \pi^*)$C=N, $(\pi \rightarrow \pi^*)$C=O, $(n \rightarrow \pi^*)$C=N and $(n \rightarrow \pi^*)$C=O, respectively which shifts in complexes toward lower wave numbers as result of coordination.

Large change is observed in the spectra of complexes with a new $n \rightarrow \pi^*$ band at 24630–42735 cm^{-1}. A tetrahedral Cu (II) complexes are rare because of Jahn-Teller effect, which causes a flattening of tetrahedron due to lifting of the degeneracy ^2T_2g ground state. Although, the Cu (II) complex under study appears to have distorted tetrahedral geometry. The diffuse reflectance spectra of Cu (II) complex show a low energy less intense band at 14450 cm^{-1} due to $d_{x2-y2} \rightarrow d_{yz}$ transition has been reported for certain Cu (II) pseudo tetrahedral geometry [26]. Also, the magnetic moment value per copper atom ($\mu_{eff.}$ =1.92 B.M.) lie within the range reported for d^9 Cu(II) ions. The visible electronic absorption spectrum of the Co(II) complex is dominated by the highest energy at 16286 cm^{-1} due to $^4A_2 \rightarrow {}^4T_1$(P) transition, which is a typical one for tetrahedral Co(II) complexes. The magnetic moment value (Table 3) as well as the green colour of complex, also suggest tetrahedral stereochemistry.

Table 3: Spectral absorption bands and the magnetic moments of H_4MDO and its metal complexes.

Compound	Band position,cm^{-1}	μ_{eff}(B.M)
H_4MDO	42735, 39682 33783, 25510	-
$[Co_2(H_2MDO)Cl_2(H_2O)_2]H_2O$	32051, 27932 23809, 16286 14749	4.67
$[Cu_2(H_2MDO)Cl_2(H_2O)_2]2H_2O$	42735, 33783 27777, 24630 14450	1.92

Thermogravimetric Studies.

The TG and DTA for solid complexes are depicted inFigs. (4 and 5). The obtained results approved the proposed formulae. Where, it is clear that the complexes decompose in three main stages. The primary stage implies the loss of hydrated water molecules at 31–90°C, followed by the loss of the coordinated water, chloride ions or acetate ions at 124–237°C. Then, the deligation process began at a temperature range of 240–800 °C and at the end, formation of metal oxide took place.

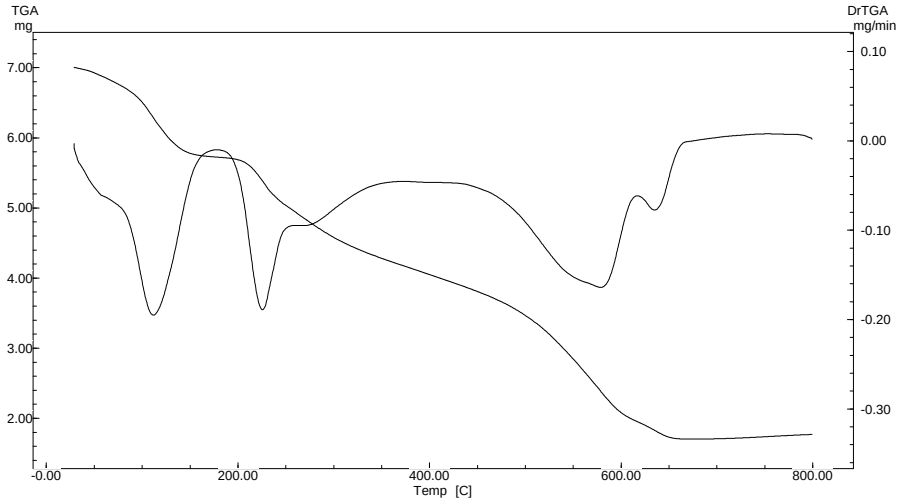

Fig. 3. Thermal analysis curves (TGA, DTG) of Co (II) complex.

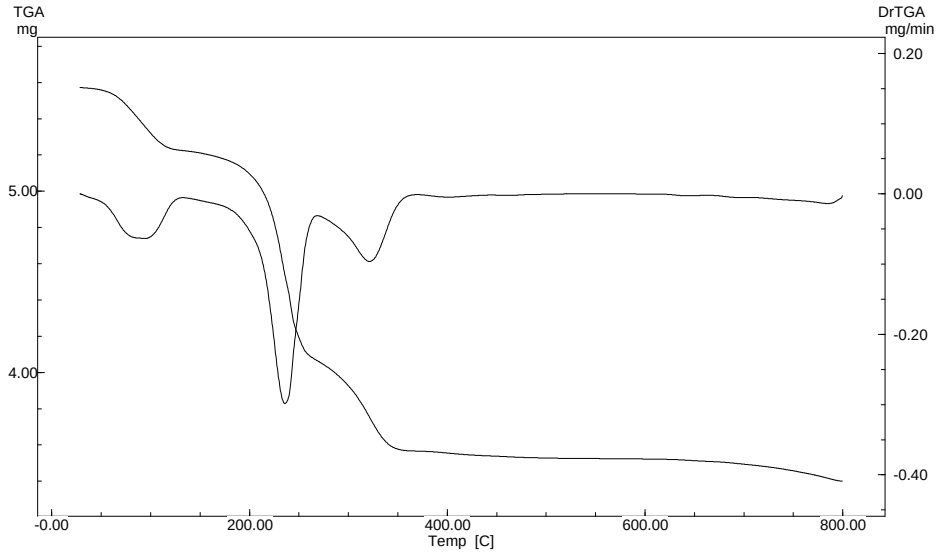

Fig. 4. Thermal analysis curves (TGA, DTG) of Cu(II) complex.

Kinetic Data of Thermal Degradation:

The kinetic parameters of decomposition stages have been evaluated by using non-isothermal methods. The rate of degradation, dα/dt, is a linear function of rate constant k (temperature dependent) and function of conversion α (temperature independent) and can be expressed as follow [a]:

$$d\alpha/dt = K(T)f(\alpha) \qquad (2)$$

The reaction rate constant, k, has been calculated by the Arrhenius expression:

$$K = Ae^{-E/RT} \qquad (3)$$

Where R is the gas constant, E is the activation energy and A is the pre-exponential factor. Substituting Eq. (3) into Eq. (2), we get:

$$d\alpha/dt = A\left(e^{-\frac{E}{RT}}\right)f(\alpha) \qquad (4)$$

When the temperature varied by a constant and controlled heating rate, Φ=dT/dt, the change in degree of conversion which is a function of temperature dependent also on time of heating. Therefore Eq. (4) becomes:

$$d\alpha/dt = A/\emptyset\left(e^{-\frac{E}{RT}}\right)f(\alpha) \qquad (5)$$

The integrated form of Eq. (5) is generally expressed as:

$$g(\alpha) = \int_0^{\alpha} \frac{d\alpha}{f(\alpha)} = A/\emptyset \int_0^{T} e^{-E/RT}\, dt \qquad (6)$$

where $g(\alpha)$ is the integrated form of the conversion dependence function. The right-hand side integral of Eq. (6) is known as temperature integral and has no closed form solution. The most used methods for evaluation of temperature integral are method of Coats-Redfern Figs. 5[27] and the approximation method of Horowitz-Metzger Figs. 6[28]. From the results obtained, the following remarks can be pointed out:

(i) The kinetic parameters (E, A, ΔH, ΔS and ΔG) of all prepared solid complexes have been calculated by CR and HM method (Table 4 and 5). The values obtained from the two methods are quite comparable.

(ii) All decomposition stages of complexes show a best fit for (n=1) suggesting a first- order decomposition in all cases. Other n values (eq.4 and 5) did not lead to better correlations.

(iii) The value of ΔG increases because the value of TΔS significantly from one stage to another which overrides the value of ΔH. Increasing the value of ΔG of a given complex on going from one decomposition step to another displayed that the rate of H_4MDO removal will be lower from step to the subsequent step [29, 30]. This may be attributed to, the structure rigidity of remaining complex after the explosion of one or more H_4MDO.

(iv) The positive value of ΔS indicates a less ordered activated complex than the reactants and /or the reactions are slow [27].

(v) The positive value of ΔH means the endothermic nature of the decomposition processes.

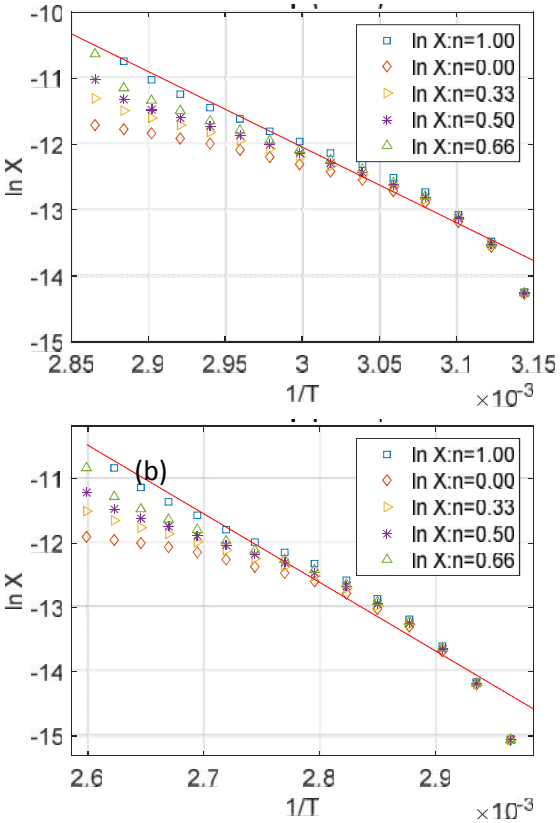

Fig.5. Coats-Redfern plot of first degradation step for (a) Co(II) complex and (b) Cu(II)complex.

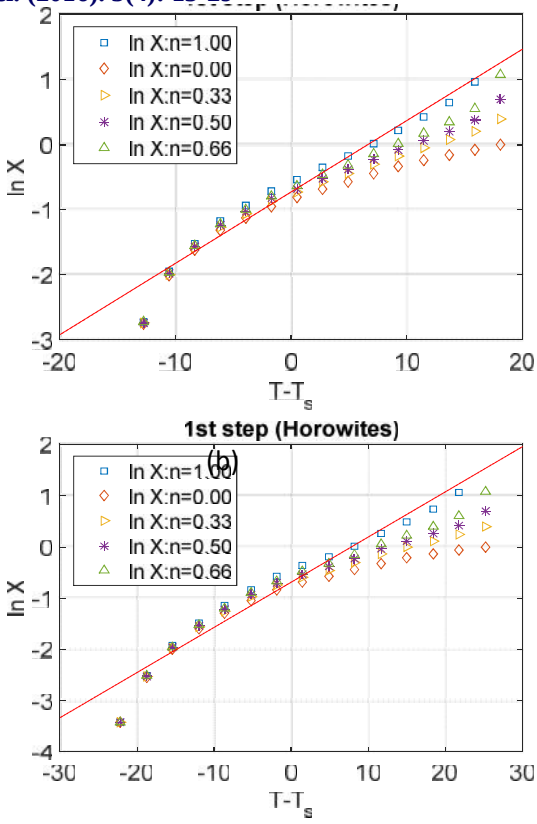

Fig.6. Horowitz-Metzger plot of first degradation step for (a) Co(II) complex and (b) Cu(II) complex.

Table 4. Kinetic Parameters evaluated by Coats-Redfern equation for the prepared complexes

Complex	peak	Mid Temp(K)	Ea KJ/mol	A (S^{-1})	ΔH* KJ/mol	ΔS* KJ/mol.K	ΔG* KJ/mol
$[Co_2(H_2MDO)Cl_2(H_2O)_2]H_2O$	1st	520.84	95.32	1.03×10^{13}	92.57	0.00336	91.46
	2nd	385.87	116.43	4.42×10^{13}	113.22	0.01418	107.75
	3rd	495.65	329.78	7.30×10^{32}	325.66	0.38000	137.31
	4th	555.32	231.13	5.86×10^{19}	226.52	0.12835	155.24
	5th	814.82	250.42	2.75×1013	243.64	0.00403	240.36
	6th	908.35	1273.28	1.76×10^{71}	1265.73	1.10972	257.71
$[Cu_2(H_2MDO)Cl_2(H_2O)_2]2H_2O$	1st	359.5	88.92	6.46×10^{10}	85.93	-0.03951	100.14
	2nd	505.29	328.57	9.26×10^{31}	324.37	0.36267	141.11
	3rd	587.02	310.84	2.48×10^{25}	305.96	0.23563	167.64

Table 5. Kinetic Parameters evaluated by Horowitz-Metzger equation for the prepared complexes**:**

Complex	peak	Mid Temp(K)	Ea KJ/mol	A (S^{-1})	ΔH* KJ/mol	ΔS* KJ/mol.K	ΔG* KJ/mol
$[Co_2(H_2MDO)Cl_2(H_2O)_2]H_2O$	1st	520.84	99.71	4.91×10^{13}	96.96	0.01633	91.56
	2nd	385.87	120.29	1.40×10^{14}	117.08	0.02374	107.92
	3rd	495.65	337.23	4.35×10^{33}	333.11	0.39483	137.41
	4th	555.32	240.14	4.03×10^{20}	235.52	0.14439	155.34
	5th	814.82	256.09	6.02×10^{13}	249.31	0.01053	240.73
	6th	908.35	1278.79	3.60×10^{71}	1271.24	1.11568	257.81
$[Cu_2(H_2MDO)Cl_2(H_2O)_2]2H_2O$	1st	359.5	94.70	4.24×10^{11}	91.71	-0.02386	100.29
	2nd	505.29	335.03	4.19×10^{32}	330.83	0.37522	141.23
	3rd	587.02	313.55	4.18×10^{25}	308.67	0.23995	167.82

Generally, the value of stepwise stability constants decreases with an increase in the number of H_4MDO attached to the metal ion [31, 32] therefore a reverse effect may occur during the decomposition process. Hence the rate of removal of the remaining H_4MDO will be lower than that of the rate before the explosion of H_4MDO.

Molecular Modeling.

The molecular structure along with atom numbering of H_4MDOand its metal complexes are shown in Structures (1- 3).From the analysis of the data calculated for the bond lengths and angles, one can conclude the following:

In both complexes increasing ofC(11)-O(13), C(5)-N(6), C(8)-O(9), N(12)-N(14) and N(14)-C(15) bond lengths with decreasing of C(11)-N(12), N(6)-N(7) and N(7)-C(8) as a result of the coordination via the (N6), O(9), N(14)and O(13) with metal atoms. The C=O bond distance in both complexes becomes longer due to the formation of the M-O bond which makes the C-O bond weaker [33] and N(6)-C(5) ,N(14)-C(15) bond distances are elonged this is referred to the formation of the M-N bond which makes the C-N bond weaker[34].

In hydrazone moiety of H_4MDO; the bond angles altered slightly after the coordination process. Where, the large change affected C(15)-N(14)-N(12), C(16)-C(15)-N(14), C(19)-C(15)-N(14), C(8)-N(7)-N(6), N(14)-N(12)-C(11), N(6)-C(5)-C(2), N(6)-C(5)-C(4), N(7)-N(6)-C(5), O(13)-C(11)-N(12) and O(9)-C(8)-N(7) angles which reduced or increased during complex formation as a consequence of bonding processes[33]. In all complexes, the bond angles lie in the range of tetrahedral geometry indicatingsp^{3}hybridization. The H_4MDO complexes can be arranged according to M-N and M-O: O(9)-Cu(23)> N(6)-Co(23)> N(14)-Cu(22)> O(13)-Cu(22)>N(14)-Co(22)>N(6)-Cu(23)>O(13)-Co(22)> O(9)-Co(23) reflecting the great strength of the Co-O and Cu-N bonds than the others. All correlates with the experimental IR frequencies. As there is an elongation in the bonds, a lower energy of the vibration frequency is needed and the lower frequency and is approved by the experimental IR frequency values. In the hydrazone backbone, the bond angles didn't change significantly, but around the metal angles undergo considerable variations after changing the metal center.

The energies of both HOMO (π donor) and LUMO (π acceptor) are main parameters in quantum chemical studies. Where, HOMO is the orbital that acts as an electron donor , LUMO is the orbital that act as the electron acceptor and these molecular orbitals are known as the frontier molecular orbitals (FMOs) Figs 7.

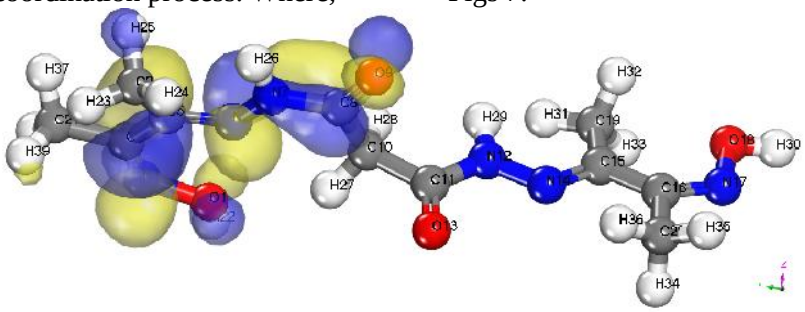

E_{LUMO}= -2.541*eV*
(excited state)

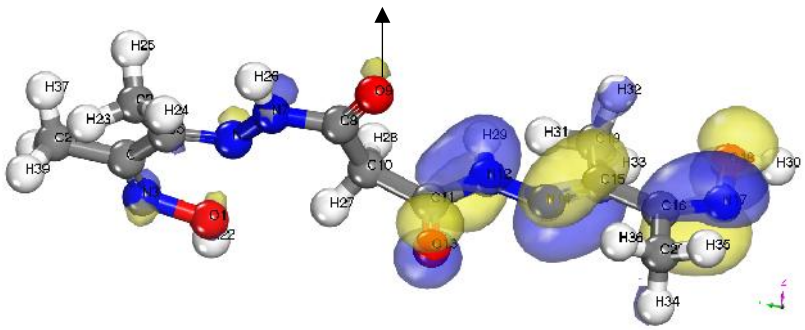

$E_{HOMO=}$ -5.190 *eV*
(ground state)

Fig. 7. 3D plots frontier orbital energies using DFT method for H_4MDO.

In many reactions, the overlap between HOMO and LUMO orbitals considered as a governing factor, where in H_4MDO; the orbitals with the higher molecular orbital coefficients can be considered as the main sites of coordination. The energy gap (E_{HOMO} - E_{LUMO}) is a significant stability index facilitate the characterization of both kinetic stability and chemical reactivity of the molecules [35]. Molecules with a small gap are known as soft molecules, they are more polarized and more reactive than hard ones because they easily offer electrons to an acceptor. In H_4MDO, the energy gap is small showing that charge transfers easily in it and this influences the biological activity of the molecule. Moreover, the low value of energy gap is due to the groups that enter into conjugation [36].

DFT method sites the selectivity of the molecular systems and concepts the chemical reactivity. The energies of frontier molecular orbitals (E_{HOMO}, E_{LUMO}), electronegativity (χ), energy band gap which explains the eventual charge transfer interaction within the molecule, global hardness (η), chemical potential (μ), global electrophilicity index (ω)and global softness (S) [37, 38] are listed in Table 6.

$$\chi = -1/2\ (E_{LUMO} + E_{HOMO}) \quad (7)$$
$$\mu = -\chi = 1/2\ (E_{LUMO} + E_{HOMO}) \quad (8)$$
$$\eta = 1/2\ (E_{LUMO} - E_{HOMO}) \quad (9)$$
$$S = 1/2\ \eta \quad (10)$$
$$\omega = \mu^2/2\ \eta \quad (11)$$

The inverse value of the global hardness is designed as the softness ϭ as follow:

$$ϭ = 1/\eta \quad (12)$$

Table 6. Calculated E_{HOMO}, E_{LUMO}, energy band gap ($E_H - E_L$), chemical potential (μ), electronegativity (χ), global hardness (η), global softness (S) and global electrophilicity index (ω) for H_4MDO and its complexes.

Compound	E_H(eV)	E_L(eV)	(E_H-E_L) (eV)	X (ev)	μ(eV)	η(eV)	S(eV^{-1})	ω (eV)	ϭ (eV)
H_2MDO	-5.190	-2.541	-2.649	3.866	-3.866	1.325	0.662	5.641	0.755
$[Co_2(H_2MDO)Cl_2(H_2O)_2]H_2O$	-4.048	-3.253	-0.795	3.651	-3.651	0.398	0.199	16.762	2.516
$[Cu_2(H_2MDO)Cl_2(H_2O)_2]2H_2O$	-4.760	-2.812	-1.948	3.786	-3.786	0.974	0.487	7.358	1.027

Ion-Flotation Separation of Cu(II):

The aim of this work was to develop a simple, sensitive and available method for the pre-concentration and determination of Cu^{2+} ions in aqueous solutions using atomic absorption spectrophotometry coupled with flotation. In this regard, the influence of various effective parameters including, pH, surfactant, metal ions and H_4MDO concentrations, temperature, as well as the effect of interference, were optimized. Numerous experiments were carried out to examine the floatability of Cu^{2+} ions using HOL as a surfactant only. The floatability of Cu^{2+} ions does not exceed 43%. Therefore, an improvement of the process was required. Trials were made using oxime derivative as chelating agent and encouragement flotation results were achieved.

Influence of pH

The solution pH is an important factor influencing flotation process since it affects not only the degree of ionization of metal ion, chelating agent and surfactant but also the speciation of the heavy metal ion in solution. Many experiments were done to study the effect of pH on the floatability of 5×10^{-5}mol L^{-1} of Cu^{2+}using 2×10^{-4}mol L^{-1} of prepared H_4MDO and 1×10^{-3}mol L^{-1} of HOL. The results attained are displayed in Fig.8. It is clear that, highest floatability of Cu^{2+} ions (~100%) was reached at the pH range 6-10, which facilitates the application of the prepared H_4MDO for the separation of Cu^{2+} ions from different media. Hence, pH ~7 was fixed for further experiments.

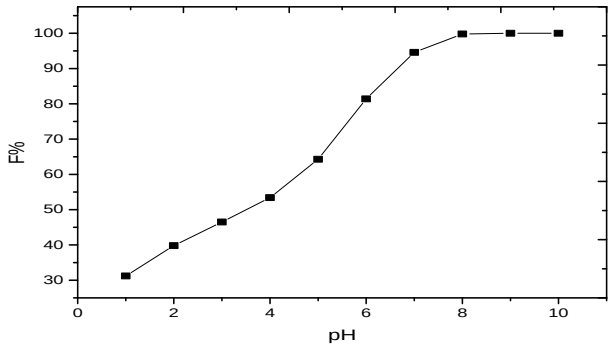

Fig. 8: Influence of pH on the floatability of 5×10^{-5}mol L^{-1} Cu^{2+} ions using 2×10^{-4}mol

Influence of Copper Concentration

Different concentrations of Cu^{2+} ions floated using 2×10^{-4}mol $L^{-1}$of H_4MDO and 1×10^{-3}mol L^{-1} HOL at pH~7. The results illustrated in fig.9 show that the maximum flotation efficiency (~100%) of Cu^{2+} ions was obtained and remained constant for the prepared H_4MDO whenever the ratio of M:L is (1:1). The chelating agent gave quantitative separation of Cu^{2+} ions (~100%) which may be attributed to the presence of sufficient amounts of prepared H_4MDO to bind all Cu^{2+} ions. Therefore, the ratio of M:L of (1:1) was used throughout.

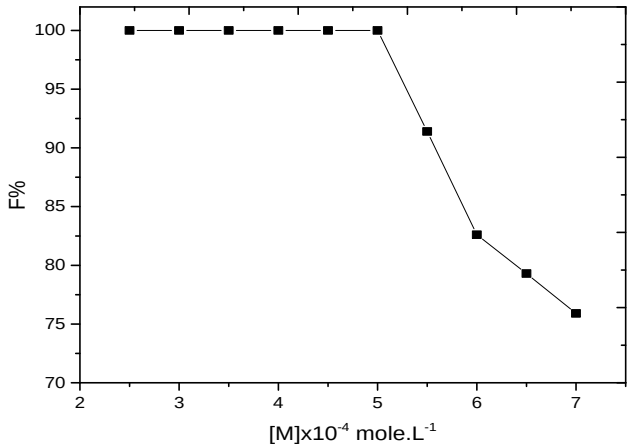

Fig. 9: Floatability of different concentrations of Cu^{2+} ions using 2×10^{-4}mol L^{-1} of prepared liugand and 1×10^{-3}mol L^{-1}HOL at pH ~7.

Influence of H_4MDO Concentration

The collecting ability of prepared H_4MDOtowards Cu^{2+} ions was tested to show the effect of different concentrations of prepared H_4MDO on the floatability of the analyte using HOL at pH ~7. The data presented in fig. 10 show that, the floatability of Cu^{2+} ions increases sharply reaching its maximum value (~100%) at M:L ratio of (1:1). Excess H_4MDO has no adverse effect on the flotation process, accordingly 2×10^{-4}mol L^{-1} of prepared H_4MDO was used throughout.

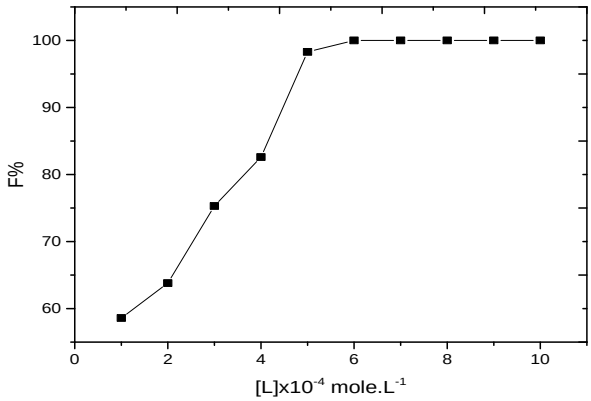

Fig. 10: Floatability of 5×10^{-5}mol L^{-1} Cu^{2+} ions using different concentrations of prepared ligand and 1×10^{-3}mol L^{-1}HOL at pH ~7.

Influence of Surfactant Concentration

Trials failed to float Cu^{2+} ions with HOL only, where the recovery did not exceed 43 %. Therefore, other experiments were performed to float 5×10^{-5}mol L^{-1} Cu^{2+} ions in the presence of 2×10^{-4}mol L^{-1} of prepared H_4MDO and different concentrations of HOL (1×10^{-3}-5×10^{-2} mol L^{-1}) at pH~7. The results illustrated in fig. 11indicate that in the HOL concentration range of 1×10^{-3}-9×10^{-3} mol L^{-1}, high floatation % of Cu^{2+} ions is achieved.

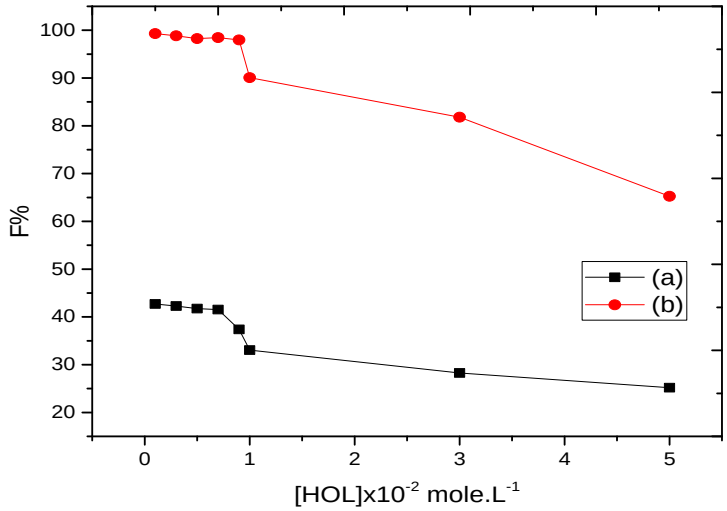

Fig. 11: Floatability of 5×10^{-5}mol L^{-1} Cu^{2+} ions using different concentrations of HOL in the presence (a) and absence (b) of 2×10^{-4}mol L^{-1} of prepared ligand at pH ~7.

At high concentrations of HOL, the decrease in separation of Cu^{2+} ions can be due to the fact that the surfactant changes the state of the particles, Cu-H_4MDOcomplex gets precipitated, from coagulation precipitation through coagulation flotation to re-dispersion with increasing the amount of HOL added[39]. Furthermore, the poor flotation at high surfactant concentration is produced by the formation on the air bubble surface of a stable, hydrated envelope of surfactant or, by forming a hydrate micelle coating on the solid surface [40, 41]. As a result, the hydrophobicity of the surface was not suitable for flotation. Therefore, a concentration of 1×10^{-3}mol L^{-1} of HOL was fixed throughout.

Influence of Temperature

A series of experiments applied to float Cu^{2+} ions at different temperatures (5-80^{o}C) under the recommended conditions. In order to do this, solution containing Cu^{2+} ions and the prepared H_4MDO and another solution containing HOL were either heated or cooled to the same temperature in a water bath. The HOL solution mixed quickly into Cu^{2+} ions solution, then the mixture introduced into the flotation cell jacketed with 1 cm thick fiberglass insulation and the flotation procedure completed. The obtained results in fig. 12 showed that maximum flotation (~100%) of Cu^{2+} ions in the range 15-65˚C. Therefore, 25˚C used throughout. At temperature higher than 80˚C, the separation decreased and this may be due to the increase in solubility of the precipitate and the instability of the foam increase the partial dissolution of the precipitate and insufficient foam consistency to hold up the precipitate [42].

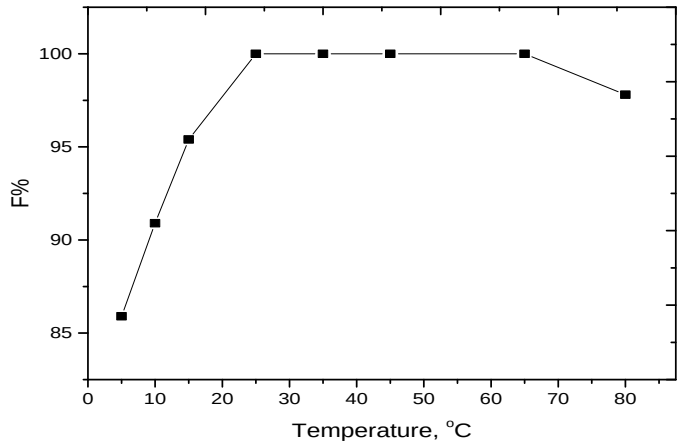

Fig. 12: Floatability of 5×10^{-5}mol L^{-1} Cu^{2+} ions at different temperatures using 2×10^{-4}mol L^{-1} of prepared ligand and 1×10^{-3}mol L^{-1}HOL at pH ~7.

Interference Study

Under optimum conditions estimated for this investigation (pH 7, 30 mg $L^{-1}H_4MDO$), the percentage of 10 mg L^{-1} Cu^{2+} ions studied in the presence of high concentrations of various cations and anions, usually present in natural water samples. All the anions used as the corresponding sodium or potassium salts whereas the cations used as their chlorides. The tolerable amounts of each ion, giving an error of ± 4% in the removal efficiency of Cu^{2+} ions are listed in table 7. Inspection of the data indicates that, the flotation of copper didn't affected by the presence of foreign ions. Consequently, the suggested procedure can be applied successfully on water samples.

Table 7: Effects of the matrix ions on the recovery percentage of the examined metal ion: [Cu = 5×10^{-5}mol L^{-1}; Ligand = 2×10^{-4}mol L^{-1}; HOL = 1×10^{-3} mol.L^{-1}; pH = 7]

Ion	Interference/analyte ratio (mgL^{-1})	Re, %
Na^+	30	100
K^+	65	98.8
Mg^{2+}	55	97.9
Ca^{2+}	35	98.9
Cl^-	24	99.1
SO_4^{2-}	14	98.8
HCO_3^-	45	98.9
CH_3COO^-	60	97.5

Application

To examine the possibility to apply of the recommended procedure, a series of experiments were applied to recover 10 mg L^{-1} of Cu(II) ions spiked to 1L from some water samples. The flotation experiments performed using 50 ml clear, uncontaminated and filtered sample solutions at pH 7. The results presented in table 8prove that the recovery was quantitative and satisfactory under the recommended conditions of the applied flotation procedure.

Table 8: Recovery of 10 mg L^{-1} of studied metal ion from some water samples: [Ligand = 1×10^{-3}mol L^{-1}; HOL = 1×10^{-3}mol L^{-1}; pH = ~7]

Water samples (location)	Cu(II) (mg L^{-1})	Re, %
Distilled water	10	99.3
Drinking water **1. (Mansoura)** **2. (Cairo)** **3. (Tanta)**	 10 10 10	 97.3 97.8 94.9
Nile water **1. (Mansoura)** **2. (Kafr El-Sheikh)**	 10 10	 98.2 88.9
Underground water (Mansoura)	10	91.95

Biological Activity

Minimum Inhibitory Concentration (MIC)

H_4MDO and its Co(II) and Cu(II) complexes were evaluated for their antibacterial activity against *Staphylococcus aureus* (*S. aureus*) as an example of Gram-positive bacteria, *Escherichia coli (E. coli)* as examples of Gram-negative bacteria and against a pathogenic *Candida albicans (C. albicans)* fungal strain. Antimicrobial and Antimycotic Activities in terms of MIC (µg/mL)in Table 9. The fungicide Fluconazole and the bactericide Ciprofloxacin were used as references to compare the potency of the tested compounds under the same conditions.

Table 9. Antimicrobial and Antimycotic Activities in terms of MIC (µg/mL).

Compound	*E. coli*	*S. aureus*	*C. albicans*
H_4MDO	9.37	6.25	2.34
Co(II) complex	3.12	1.17	0.58
Cu(II) complex	75	50	25
Ciprofloxacin	1.56	0.78	----
Fluconazole	----	----	1.17

H_4MDO have an acceptable activity with MIC 9.37, 6.25 and 2.34 µg/mL for *E.coli*, *S. aureus* and *C. albicans*, respectively. Furthermore, Co(II) complex is the most potent against *Staphylococcus aureus* (*S. aureus*), *Escherichia coli (E. coli)* and *Candida albicans (C. albicans)* based on the reference compounds activities with MIC 1.17, 3.12 and 0.58 µg/mL, respectively. On the other hand, Cu(II) complex shows the lowest activities.

Cytotoxicity Assay

In our experiments, IC_{50} values (compound concentration that produces 50% of cell death) in micro molar units were calculated. For comparison purposes the cytotoxicity of Fluorouracil (5-FU) and the free H_4MDO as well as its complexes has been evaluated under the same experimental conditions. It is clearly observed that chelation with metal has no synergistic effect on the cytotoxicity. Importantly, it should be emphasized that H_4MDO show strong activity nearly to that of Fluorouracil (15.10 µmol/L) for (HePG-2). These gratifying results are encouraging its further screening in vitro. Later on, upon further analysis, this H_4MDO also exhibits considerable cell growth inhibition activity against human liver hepatocellular carcinoma (HePG-2) cells. Therefore, its further biological evaluation in vivo as well as studies of mechanism of action is necessary [13].

From Table 10, the tested human tumor cells of hepatocellular carcinoma (HePG-2) fig. 13, Show greater response with the Co(II) complex than prepared ligand H_4MDO. But Cu(II) complex show moderate results of IC_{50} (µmol/L) = 53.0 against (HePG-2).

Table 10. *In vitro* Cytotoxicity IC50 activity of H_4MDO and its metal complexes against human tumor cells hepatocellular carcinoma (HePG-2)

Compound	***In vitro* Cytotoxicity IC_{50} (µmol/L)**
	HePG-2
5-Fu	7.9±0.84
H_4MDO	15.1±1.18
Co(II) complex	5.6±0.53
Cu(II) complex	53.0±4.30

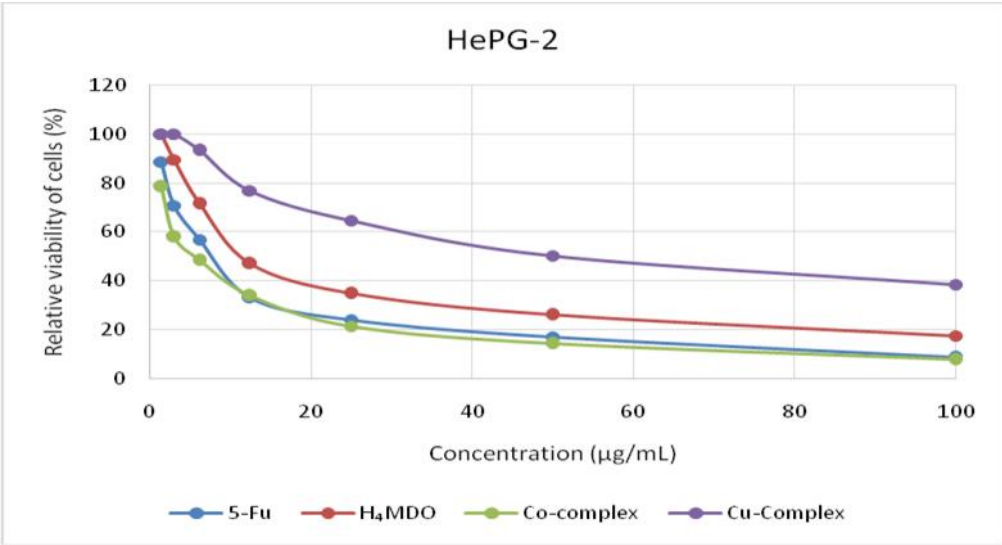

Fig. 13.Relative viability of tumor cells with concentration of H_4MDO and its complexes

Conclusion

The oxime hydrazone derived from the condensation of malonohydrazide with diacetyl monoxime and its Co(II) and Cu(II) complexes were prepared.IR spectra suggest that the H_4MDObehaves as binegativetetradentate in both complexes.The electronic spectral data of the complexes as well as their magnetic moment values suggest tetrahedral geometries for all isolated complexes. The ion-flotation oxime derivative as organic chelate for the separation of about 100% of Cu^{2+} ions procedure is free from interferences, does not affected by raising temperature up to 65˚C (which giving a chance for application to hot wastewater without need for cooling) making the process economic. Co(II)complex show higher Minimum inhibitory concentration (MIC) activity than H_4MDO and Cu(II) complex. While, the Cytotoxicity assay revealed the higher activity of H_4MDO and Co(II) complex than Cu(II) complex.

References

[1] El-Asmy, A. A., Al-Ansi, T. Y., Amin, R. R., and El-Shahat, F. 1990. Structural studies on cadmium (II), cobalt (II), copper (II), nickel (II) and zinc (II) complexes of 1-malonyl-bis (4-phenylthiosemicarbazide), *Transition Met. Chem.15*, 12-15.

[2] El-Asmy, A. A., El-Gammal, O., Radwan, H., and Ghazy, S. 2010. Ligational, analytical and biological applications on oxalyl bis (3, 4-dihydroxybenzylidene) hydrazone, *Spectrochim. Acta. A Mol. Biomol. Spectrosc.77*, 297-303.

[3] Terra, L. H. S. Á., da Cunha Areias, M. C., Gaubeur, I., Encarnación, M., and Suárez-Iha, V. 1999. Solvent extraction-spectrophotometric determination of nickel (II) in natural waters using di-2-pyridyl ketone benzoylhydrazone, *Spectrosc. Lett.32*, 257-271.

[4] Stoica, L., Dinculescu, M., and Plapcianu, C. G. 1998. Mn (II) recovery from aqueous systems by flotation, *Water Res.32*, 3021-3030.

[5] Doyle, F. M., and Liu, Z. 2003. The effect of triethylenetetraamine (Trien) on the ion flotation of Cu 2+ and Ni 2+, *J. Colloid Interface Sci.258*, 396-403.

[6] Viñuelas-Zahínos, E., Maldonado-Rogado, M., Luna-Giles, F., and Barros-García, F. 2008. Coordination behaviour of Schiff base 2-acetyl-2-thiazoline hydrazone (ATH) towards cobalt (II), nickel (II) and copper (II), *Polyhedron27*, 879-886.

[7] Vicini, P., Zani, F., Cozzini, P., and Doytchinova, I. 2002. Hydrazones of 1, 2-benzisothiazole hydrazides: synthesis, antimicrobial activity and QSAR investigations, *Eur. J. Med. Chem.37*, 553-564.

[8] Bernhardt, P. V., Mattsson, J., and Richardson, D. R. 2006. Complexes of cytotoxic chelators from the dipyridyl ketone isonicotinoyl hydrazone (HPKIH) analogues, *Inorg. Chem.45*, 752-760.

[9] Iskander, M. F., El-Sayed, L., Salem, N. M., Haase, W., Linder, H. J., and Foro, S. 2004. Synthesis, characterization and magnetochemical studies of some copper (II) complexes derived from n-salicylidene-n-alkanoylhydrazins: X-ray crystal and molecular structure of bis [monochloro-(μ-n-salicylidenemyristoylhydrazine) ono (−1)] dicopper (II), *Polyhedron23*, 23-31.

[10] Kaymakçıoğlu, B. K., and Rollas, S. 2002. Synthesis, characterization and evaluation of antituberculosis activity of some hydrazones, *Il Farmaco57*, 595-599.

[11] Patole, J., Sandbhor, U., Padhye, S., Deobagkar, D. N., Anson, C. E., and Powell, A. 2003. Structural chemistry and in vitro antitubercular activity of acetylpyridine benzoyl hydrazone and its copper complex against Mycobacterium smegmatis, *Bioorg. Med. Chem. Lett.13*, 51-55.

[12] Yousef, T., Rakha, T., El Ayaan, U., and El Reash, G. A. 2012. Synthesis, spectroscopic characterization and thermal behavior of metal complexes formed with (Z)-2-oxo-2-(2-(2-oxoindolin-3-ylidene) hydrazinyl)-N-phenylacetamide (H_2OI), *J. Mol. Struct.1007*, 146-157.

[13] Yousef, T., El-Reash, G. A., El-Gammal, O., and Ahmed, S. F. 2014. Structural, DFT and biological studies on Cu (II) complexes of semi and thiosemicarbazide ligands derived from diketo hydrazide, *Polyhedron81*, 749-763.

[14] Vogel, A. I. 1991. *Vogel'sTextbook of Quantitative Chemical Analysis*, 5th ed., Longmans, London.

[15] Ghazy, S. E., and Kabil, M. A. 1994. Determination of Trace Copper in Natural Waters after Selective Separation by Flotation, *Bull. Chem. Soc. Jpn.67*, 2098-2102.

[16] Hawkey, P., and Lewis, D. 1994. *Medical Bacteriology—A Practical Approach*, Oxford University Press, United Kingdom.

[17] Mosmann, T. 1983. Rapid colorimetric assay for cellular growth and survival: application to proliferation and cytotoxicity assays, *J. Immunol. Methods65*, 55-63.

[18] Mauceri, H. J., Hanna, N. N., Beckett, M. A., Gorski, D. H., Staba, M.-J., Stellato, K. A., Bigelow, K., Heimann, R., Gately, S., and Dhanabal, M. 1998. Combined effects of angiostatin and ionizing radiation in antitumour therapy, *Nature394*, 287-291.

[19] Delley, B. 2002. Hardness conserving semilocal pseudopotentials, *Phys. Rev. B: Condens. Matter66*, 155125.

[20] Modeling and Simulation Solutions for Chemicals and Materials Research, Materials Studio, *Version 7.0*, Accelrys software Inc., San Diego, USA (2011).

[21] Hehre, W. J. 1986. *Ab initio molecular orbital theory*, Wiley-Interscience.

[22] Kessi, A., and Delley, B. 1998. Density functional crystal vs. cluster models as applied to zeolites, *Int. J. Quantum Chem68*, 135-144.

[23] Matveev, A., Staufer, M., Mayer, M., and Rösch, N. 1999. Density functional study of small molecules and transition-metal carbonyls using revised PBE functionals, *Int. J. Quantum Chem75*, 863-873.

[24] Hammer, B., Hansen, L. B., and Nørskov, J. K. 1999. Improved adsorption energetics within density-functional theory using revised Perdew-Burke-Ernzerhof functionals, *Phys. Rev. B: Condens. Matter59*, 7413.

[25] Madden, D., and Nelson, S. 1968. The Co-ordination number of transition-metal ions. Part VI. Four-and five-co-ordinate complexes of some bivalent metal ions with bis-[2-(2-pyridyl) ethyl] amine, *J. Chem. Soc. A*, 2342-2348.

[26] Patil, R. M. 2007. Synthetic, structural and biological properties of binuclear complexes with some schiff bases, *Acta Pol. Pharm. Drug Res64*, 345-353.

[27] Moore, J. W., and Pearson, R. G. 1961. *Kinetics and mechanism*, John Wiley & Sons, New York.

[28] Hatakeyama, T., and Quinn, F. 1994. Fundamentals and applications to polymer science, *J. Therm. Anal.*

[29] Maravalli, P., and Goudar, T. 1999. Thermal and spectral studies of 3-N-methyl-morpholino-4-amino-5-mercapto-1, 2, 4-triazole and 3-N-methyl-piperidino-4-amino-5-mercapto-1, 2, 4-triazole complexes of cobalt (II), nickel (II) and copper (II), *Thermochim. Acta325*, 35-41.

[30] Yusuff, K. M., and Sreekala, R. 1990. Thermal and spectral studies of 1-benzyl-2-phenylbenzimidazole complexes of cobalt (II), *Thermochim. Acta159*, 357-368.

[31] Siddalingaiah, A. H. M., and Naik, S. G. 2002. Spectroscopic and thermogravimetric studies on Ni(II), Cu(II) and Zn(II) complexes of di(2,6-dichlorophenyl)carbazone, *J. Mol. Struct. THEOCHEM582*, 129-136.

[32] Chacko, J., and Parameswaran, G. 1984. Thermal decomposition kinetics of vanillidene anthranilic acid complexes of cobalt (II), nickel (II), copper (II) and zinc (II), *J. Therm. Anal. Calorim.29*, 3-11.

[33] West, D. X., Swearingen, J. K., Valdés-Martínez, J., Hernández-Ortega, S., El-Sawaf, A. K., van Meurs, F., Castiñeiras, A., Garcia, I., and Bermejo, E. 1999. Spectral and structural studies of iron (III), cobalt (II, III) and nickel (II) complexes of 2-pyridineformamide N (4)-methylthiosemicarbazone, *Polyhedron18*, 2919-2929.

[34] Despaigne, A. A. R., Da Silva, J. G., Do Carmo, A. C. M., Piro, O. E., Castellano, E. E., and Beraldo, H. 2009. Copper (II) and zinc (II) complexes with 2-benzoylpyridine-methyl hydrazone, *J. Mol. Struct.920*, 97-102.

[35] Govindarajan, M., Periandy, S., and Carthigayen, K. 2012. FT-IR and FT-Raman spectra, thermo dynamical behavior, HOMO and LUMO, UV, NLO properties, computed frequency estimation analysis and electronic structure calculations on α-bromotoluene, *Spectrochim. Acta. A Mol. Biomol. Spectrosc.97*, 411-422.

[36] Abu El-Reash, G. M., El-Gammal, O., Ghazy, S., and Radwan, A. 2013. Characterization and biological studies on Co (II), Ni (II) and Cu (II) complexes of carbohydrazones ending by pyridyl ring, *Spectrochim. Acta. A Mol. Biomol. Spectrosc.104*, 26-34.

[37] Pearson, R. G. 1989. Absolute electronegativity and hardness: applications to organic chemistry, *J. Org. Chem.54*, 1423-1430.

[38] Padmanabhan, J., Parthasarathi, R., Subramanian, V., and Chattaraj, P. 2007. Electrophilicity-based charge transfer descriptor, *J. Phys. Chem. A111*, 1358-1361.

[39] Ghazy, S. E.-S., Samra, S. E.-S., Mahdy, A. E.-F. M., and EL-MORSY, S. M. 2006. Removal of aluminum from some water samples by sorptive-flotation using powdered modified activated carbon as a sorbent and oleic acid as a surfactant, *Anal. Sci.22*, 377-382.

[40] Klassen, V. I., and Mokrousov, V. A. 1963. *An introduction to the theory of flotation*, Butterworths.

[41] Ghazy, S. E.-S., and Moustafa, G. A.-H. 2001. Flotation-Separation of Chromium (VI) and Chromium (III) from Water and Leathers Tanning Waste Using Active Charcoal and Oleic Acid Surfactant, *Bull. Chem. Soc. Jpn.74*, 1273-1278.

[42] Ghazy, S., Rakha, T., El-Kady, E., and El-Asmy, A. 2000. Use of some hydrazine derivatives for the separation of mercury (II) from aqueous solutions by flotation technique, *Indian J. Chem. Technol.7*, 178-182.

.

Access this Article in Online	
	Website: www.ijarbs.com
Quick Response Code	**Subject:** Chemistry

How to cite this article:

Hany M. Youssef, Mohammed M. El-Gamil, YasirKh. Abdulhamed, Gaber M. Abu El-Reash. (2016). Co(II) and Cu(II) complexes of oxime hydrazone derivative: Structural, geometrical, biological studies andion-flotation separation of Cu(II) ions.. Int. J. Adv. Res. Biol. Sci. 3(4): 13-29.